IOSR Journal of Mechanical and Civil Engineering (IOSR-JMCE)
e-ISSN: 2278-1684,p-ISSN: 2320-334X, Volume 15, Issue 4 Ver. V (Jul. - Aug. 2018), PP 19-25
www.iosrjournals.org

Simulation of Flows over an Air-Regulated Siphon Spillway

Prasanna S V S N D L[1], Suresh Kumar N[2]
[1,2] *(Department Civil Engineering, College of Engineering (A), Osmania University, Hyderabad – 500007, Telangana State, India)*

Abstract: *The air-regulated siphon spillways are adopted on streams that are subjected to flash floods or where there is insufficient space to provide conventional weirs. Discharge in an air – regulated spillway is solely governed by the area of the waterway at throat section. Air – regulated siphon spillway work automatically for a wide range of discharges even for a small rise in the upstream water level, without any mechanical or human interference. The physical model of air-regulated siphon was made of acrylic and mounted in a glass sided channel at RGKUT, Basar. The present work focuses on the experimental studies carried out for various discharges ranging from 4.3 lps to 7.2 lps. The simulation studies were carried out using ANSYS-CFD. The simulations were extended to determine the flow pattern and the free surface level on the upstream and downstream of the siphon in the flume. The user-defined macro was generated to evaluate the flow pattern upstream, at the crest level of the siphon and downstream of the air-regulated siphon spillway. The comparative analysis proved that the Fluent software is a powerful tool in evaluating the flow properties of the model even in the absence of physical modeling.*

Keywords: - *Air-regulated siphon, Flow pattern, Fluent, k-ε/k-ω, User-defined macro*

Date of Submission: 12-07-2018 Date of acceptance: 26-07-2018

I. Introduction

Siphons are of great fascination to any hydraulic engineer. These are adopted for low-head capacity installations, where the reservoir fluctuations are reasonably small. It is also advisable under large installations, to dispose-off huge flood waters. In circumstances where the siphoning action is essential, they are mostly closed conduit accompanied by an inlet, an upward sloping section, a crown with a level crest section, a downward sloping section, and an outlet. The water is discharged onto the downstream side through the siphoning action, instead of allowing it to spill over the crest over the spillway. In siphons, water is allowed to flow to the downstream side when the upstream water level rises over the crest. The air-regulated siphons are said to draw continuous air flow that controls the discharge in combination with the water to form a white-water stream. This is safer than the black water in which the head of the stream causes the increase in the discharge to a maximum level, once the siphon is primed. This siphon works on an on-off principle, with the maximum and minimum discharge flow levels fluctuating at the intake. Another advantage of air-regulated spillway is that, it eliminates the hunting and vibration problems that are associated in many black water siphons [1].

An air regulated siphon was first designed by Crump and was constructed in late 1922 at Renala. Since 1960, the use of air regulated siphon spillway increased considerably as a flood control measure, in hydro-electric power systems, etc. With the day-to-day increase in the technology, the operational principles have been well understood by the hydraulic engineers. However, the research is still in progress to understand the clear utilization of siphon spillways. In brief perceptive, the air regulated spillways are designed in two different cases viz., with a free outlet, when a ski-jump is required to facilitate the air evacuation process and with a nappe deflector, when the exit is sealed by the tail water. In the above two cases, the air in the siphon is entrained thereby causing a pressure drop.

The air regulated spillways operate securely at any discharge with a slight variation in the upstream level. Further, these siphons are helpful in reducing the spillway width. Moreover, the unique feature of the air-regulates siphon is that, the entire operation is carried out automatically without any mechanical or personal interference [2]. When the flow of a liquid occurs over the spillway crest, the resulting motion is a free vortex flow. By substituting the rate of an external torque equal to zero or the time rate of change of angular momentum equal to zero, it is possible to obtain a relation between velocity and radii (v.r = constant). An air-regulated siphon operation is divided into four distinct stages as detailed below:

Weir Flow: The rise in water level on the upstream side makes the water to flow over the crest and slowly moves towards the downstream side of the siphon. As the water level is below the upper lip, the air that is relinquished will be immediately replaced. This pressure in the channel will be still atmospheric. This phase of flow is termed as conventional weir flow.

Deflected Flow: When there is an increase in the level of water, the air passage under the lip is completely arrested. The siphon container is sealed and becomes free from atmospheric pressure. In the process of evacuation of air, a partial vacuum is produced. This leads to rise in the head of water above the crest leading to increase in discharge. This, in turn decreases the level of water in the environs of the upstream lip. Therefore, air is sucked into the siphon to recompensate for the extraction at the downstream end. This is not a recurring process, but is continuous as air and water are drawn continuously into the siphon. This phenomenon of rise in the water level on the upstream side eventually reduces the inflow of air, leading to increase in the discharge. Similarly, when there is fall in water level, the discharge gets reduced. This process clearly demonstrates that the siphon is self – regulating. For any increased discharge, the nappe gets depressed by the momentum of water passing down the glacis and drowned by the rising of tail water.

Air-Partialized Flow: With the continuous increase in flow, the water level will rise within the hood to the degree leading to disappearance of the low-pressure. In this situation, the siphon barrel flows full and is completely occupied by a mixture of air and water. The siphon is then said to be air – partialized. During this phase, the nature of flow completely changes and full influence of tail water is observed, possibly making it difficult to analyze.

Blackwater Flow: This is a condition having maximum rise in the water level with full discharge capacities on the upstream side. The siphon hood flows full with no air in the system [3]. The use of air-regulated siphon spillway is witnessed to have significant benefits in most of the hydraulic structures without any manual effort.

Many authors in the past have discussed on the suitability design and evaluated certain characteristics of air-regulated siphon spillway. Joshua Boatwright (2014) experimentally evaluated the performance of air-regulated siphon to quantify the flow rates and vent sizes. A validation study was also carried out with the data available on 40 year old water column structure at LaMaster Diary farm installed at Clemson University. The author further carried out cost analysis for framing guidelines for the installation of siphon spillway [4]. Christopher (1975) studied the behavior of low-head air regulated siphons based on the stage-discharge curves. The author conducted experiments on two siphon models of 1:10 scale, of 150mm wide flume constructed of timber and plastic. From the analysis, the author recommended that the low-head siphons shall be simple in design and undistorted. The discussion also stated that, special care should be taken in deciding the crest level along with other features of the siphon spillway [5].

The present investigation was carried out to experimentally investigate the height and plot the flow profile passing through upstream, crest level and downstream side of siphon. The simulation and validation of the experimental results was carried out using the modeling technique viz., ANSYS-CFD (Fluent). This research is another step to understand the wide applicability of the Computational Fluid Dynamics as a best numerical technique.

II. Material And Methods

The experiments were carried out in the Fluid Mechanics Laboratory of Department of Civil Engineering, Rajiv Gandhi University of Knowledge Technologies (RGUKT), Basar. The tilting flume is of 5.0 m long with the cross section of 0.3 m width and 0.46 m height. It is equipped with a reservoir on the upstream side, forming the entrance of the channel for generating a uniform flow in the channel. The water into the channel was re-circulated using a pump. The longitudinal section of the siphon is shown in Fig.1. The channel is having an aluminum base with glass sided walls enabling a clear view of the flow through the channel. The two movable point gauges were mounted on the top of the channel sides by means of a mechanical adjustment. The detachable air regulated spillway was made from acrylic material as shown in the Fig. 2. The siphon spillway is 0.3m wide, 0.303m in length and 0.255m height. The siphon was mounted in between the walls of the channel, at a distance of 2.0m downstream of the inlet in the tilting flume. The actual discharge estimations were made by direct weight measurement of water. The water surface levels in the channel were measured by using point gauges of 0.1mm precision. The present investigations were carried out for four different discharges varying from 4.3 lps to 7.3 lps. The depth of the flow on the upstream and downstream of the siphon spillway is detailed in the TABLE 1.

In the present study, the turbulence involved in the siphon spillways was captured using Fluent software by the adoption of k-Epsilon and k-Omega turbulence models. For the two dimensional steady state incompressible flow, the Reynolds-averaged Navier-Stokes equations are given below [6]:

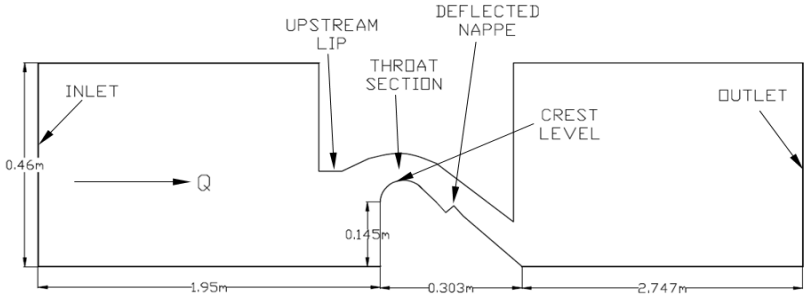

Fig no 1 Longitudinal section of Siphon

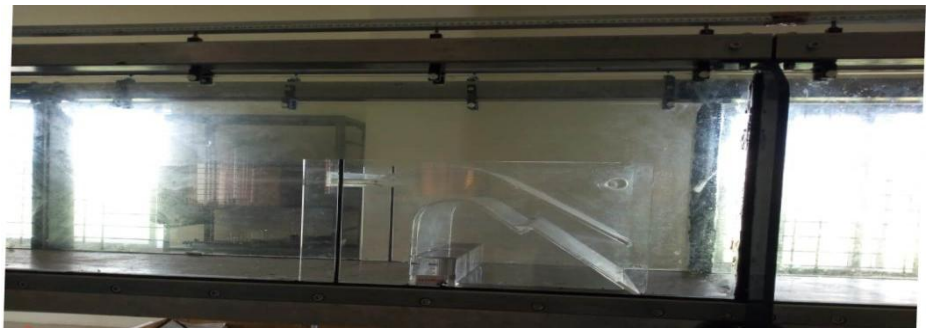

Fig no 2 Siphon spillway from arcylic material in flume

Table no 1 Experimental Results

S. No	Discharge Q	Approach Velocity V_a	Upstream depth Y_1	Downstream depth Y_2
	cumec ($\times 10^{-3}$)	m/s	m	m
1	4.3	0.063	0.229	0.0156
2	5.3	0.073	0.240	0.0175
3	6.3	0.081	0.247	0.018
4	7.2	0.096	0.252	0.0218

$$\frac{\partial \bar{u}}{\partial x}+\frac{\partial \bar{v}}{\partial y}=0 \quad \text{..... (1)}$$

$$\rho\left(\bar{u}\frac{\partial \bar{u}}{\partial x}+\bar{v}\frac{\partial \bar{u}}{\partial y}\right)=-\frac{\partial \bar{p}}{\partial x}+\frac{\partial}{\partial x}\left(\mu\frac{\partial \bar{u}}{\partial x}-\rho\overline{u'u'}\right)+\frac{\partial}{\partial y}\left(\mu\frac{\partial \bar{u}}{\partial y}-\rho\overline{u'v'}\right) \quad \text{..... (2)}$$

$$\rho\left(\bar{u}\frac{\partial \bar{v}}{\partial x}+\bar{v}\frac{\partial \bar{v}}{\partial y}\right)=-\frac{\partial \bar{p}}{\partial y}+\frac{\partial}{\partial x}\left(\mu\frac{\partial \bar{v}}{\partial x}-\rho\overline{u'v'}\right)+\frac{\partial}{\partial y}\left(\mu\frac{\partial \bar{v}}{\partial y}-\rho\overline{v'v'}\right) \quad \text{..... (3)}$$

In the equation – 2 & 3, the terms $-\rho\overline{u'u'}$, $-\rho\overline{v'v'}$ and $-\rho\overline{u'v'}$ behave like stress terms, the first two terms are normal stresses and the last term is a shear stress. The process of finding a closure to the system of equations incorporated is known as Turbulence Modeling. In the CFD, two approaches are commonly adopted viz., second moment closure approach for solving the transport equations and the turbulent viscosity approach. The second approach involves solving two differential equations, one representing the generation of transport of turbulence and the other representing the transport of dissipation of turbulence viz., k - ε and k – ω models.

Turbulence Kinetic Energy (k-ε model) [7]:

$$\frac{\partial k}{\partial t}+U_j\frac{\partial k}{\partial x_j}=\tau_{ij}\frac{\partial U_i}{\partial x_j}-\varepsilon+\frac{\partial}{\partial x_j}\left[\left(\nu+\nu_T/\sigma_k\right)\frac{\partial k}{\partial x_j}\right] \quad \text{..... (4)}$$

The first term on the LHS of eqn. (4) represents the rate of change of k or ε and the second term explains the transport of k or ε by convection. While the first term on the RHS symbolizes the rate of production of k or ε, the second term demonstrates the rate of destruction of k or ε and the third term illustrates the transport of k or ε by diffusion.

Dissipation Rate:

$$\frac{\partial \varepsilon}{\partial t} + U_j \frac{\partial \varepsilon}{\partial x_j} = C_{e1} \frac{\varepsilon}{k} \tau_{il} \frac{\partial U_i}{\partial x_j} - C_{e2} \frac{\varepsilon^2}{k} + \frac{\partial}{\partial x_j} \left[\left(\nu + \nu_T / \sigma_\varepsilon \right) \frac{\partial k}{\partial x_j} \right] \text{..... (5)}$$

The production and the dissipation terms of eq. 5 are formed from the production and dissipation terms of the turbulent kinetic energy eq. 4 scaled by ε/k and multiplied by empirically determined constants and wall damping functions (C_{e1} and C_{e2}). An additional damping function must be included for the eddy viscosity in the k-ε equation by near walls so that k and ε will have the proper behavior in the near region.
Closure coefficients and auxiliary relations are given below:
$C_{e1} = 1.44$, $C_{e2} = 1.92$, $\sigma_k = 1.0$, $\sigma_\varepsilon = 1.3$, $\omega = \varepsilon/(C_\mu k)$
Where, k - Kinetic energy of turbulent fluctuations per unit mass, U_i - Mean velocity in tensor notation, ν_T - Kinematic eddy viscosity, ν - Kinematic molecular viscosity, τ_{ij} - Specific Reynolds stress tensor

Turbulent kinetic energy (k-ω model)

$$\frac{\partial \mathrm{k}}{\partial \mathrm{t}} + \mathrm{U_j} \frac{\partial \mathrm{k}}{\partial \mathrm{x_j}} = \tau_{\mathrm{ij}} \frac{\partial \mathrm{U_i}}{\partial \mathrm{x_j}} - \beta^* \mathrm{k}\omega + \frac{\partial}{\partial \mathrm{x_j}} \left[\left(\mathrm{v} + \sigma^* \frac{\mathrm{k}}{\omega} \right) \frac{\partial \mathrm{k}}{\partial \mathrm{x_j}} \right] \text{..... (6)}$$

Specific Dissipation Rate:

$$\frac{\partial \omega}{\partial t} + U_j \frac{\partial \omega}{\partial x_j} = \alpha \frac{\omega}{k} \tau_{ij} \frac{\partial U_i}{\partial x_j} - \beta \omega^2 + \frac{\sigma_d}{\omega} \frac{\partial k}{\partial x_j} \frac{\partial \omega}{\partial x_j} \left[\left(\nu + \sigma \frac{k}{\omega} \right) \frac{\partial \omega}{\partial x_j} \right] \text{..... (7)}$$

Closure coefficients and auxiliary relations

$\alpha = 13/25$, $\beta = \beta_o f_B$, $\beta^* = 9/100$, $\sigma = 0.5$, $\sigma^* = 3/5$, $\sigma_d = \begin{cases} 0, \frac{\partial k}{\partial x_j} \frac{\partial \omega}{\partial x_j} \le 0 \\ \sigma_{do}, \frac{\partial k}{\partial x_j} \frac{\partial \omega}{\partial x_j} > 0 \end{cases}$

The semi-implicit method for pressure – linked coupling, was adopted which is designed exclusively for turbulence simulations. Each trial run was solved for various equations such as Continuity, X - Velocity, Y - Velocity, k – equation and ε / ω – equation leading to convergence.

The geometry and the mesh were generated in the Gambit. The mesh was made of 0.01 cell size and 25067 number of nodes of Quadra-triangular cells as shown in the Fig. 3. The minimum orthogonal quality of the mesh was 0.759. The mesh was imported into fluent and the simulation was conceded out for various discharges using multi phase analysis by means of Finite Volume Method (FVM). The boundary conditions adopted were: velocity inlet upstream of the air-regulated spillway, pressure outlet on the downstream end of the flume, as well as for the top of the flume on both the sides of the spillway, and wall for the rest of the boundaries of the geometry. For all the simulations consisting of free surface flows, the interface between water and air is very crucial. Therefore, it was appropriate to use the VOF model because the interface cell can be tracked as a mixture cell. All properties are shared by the phases and represent volume-averaged values in a single cell consisting mixture. In the present case, based on the concept of volume fraction, mainly two properties were shared viz., velocity and pressure in the present case. The total volume fractions of all phases pertaining to each domain cell amounts to unity in which the cell density was calculated using the equation (8).

$$\rho = \alpha_w \rho_w + \alpha_a \rho_a = \alpha_w \rho_w + (1 - \alpha_w) \rho_a \text{ ..... (8)}$$

Where, ρ is the cell density (kg/m^3); α_w is volume fraction of water in %; ρ_w is density of water in (kg/m^3); α_a is volume fraction of air in %; ρ_a is the density of air (kg/m^3).

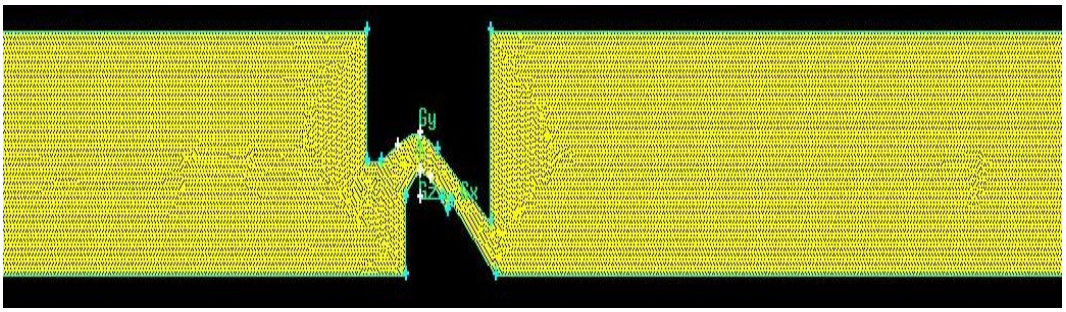

Fig no 3 mesh generated in Gambit

Each flow is analyzed for a time step of 0.01s for a maximum of 2500 time steps. The convergence was found nearly after 25s, with more than 20,000 iterations as shown in the Fig. 4. The runtime took a maximum of 3 to 4hrs of computer time for the solution to convergence.

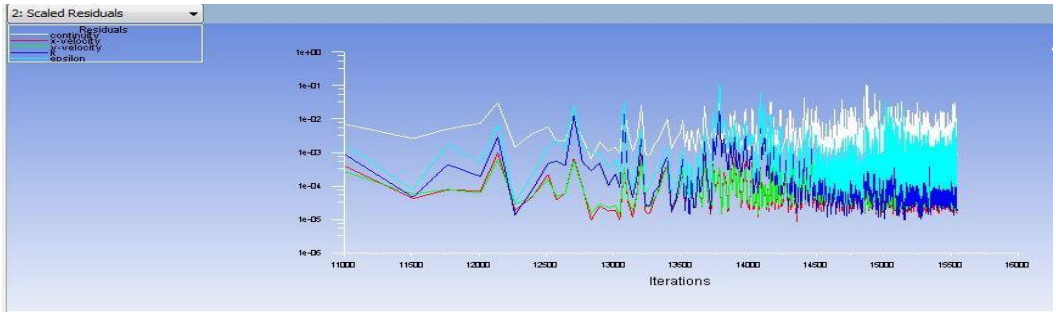

Fig no 4 Iteration Graph

The contours of multi phases viz., water, with volume fraction as '1'; air with volume fraction as '0' and in mixture between 0 and 1 as shown in the Fig. 5. The velocity magnitude profiles were plotted using Graphics and Animations and were observed to have same pattern as that observed in experimental analysis.

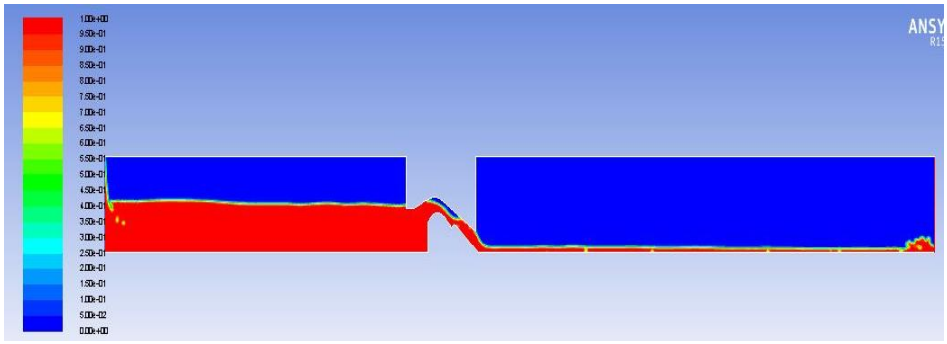

Fig no 5 Contours of Volume Fraction for 0.063m/s

The simulation was carried out by means of a User Defined Function (UDF). The UDF evaluates the shape of the profile defining the depth on the upstream and downstream of the siphon spillway. The macros featuring the volume fractions at various cell points beginning from the entrance of the channel were programmed. The programme was executed in the Fluent solver in order to obtain all the depth variations and volume fraction values at the corresponding cells both upstream and downstream of the siphon. The path traced by the flow over the siphon spillway as indicated by the numerical simulation is shown in Fig. 6.

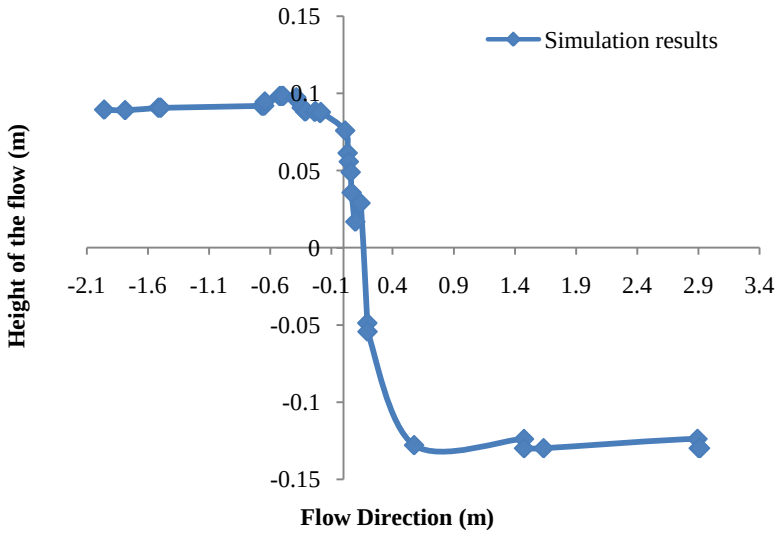

Fig no 6 Simulated Free Surface Pattern

III. Result and Discussions

1. The experiments were conducted to analyse the different phases arising from the variation of flow ranging from 4.3 lps to 7.2 lps.
2. Two types of flow phases were observed in experimental analysis via. weir flow, and deflected nappe as detailed in TABLE 2.

Table no 2 Flow phases of Air – Regulated Spillway

S. No	Discharge Q	Approach Velocity V_a	Type of Flow
	cumec (x 10^{-3})	m/s	
1	4.3	0.063	Weir Flow
2	5.3	0.073	Deflected Nappe
3	6.3	0.081	Deflected Nappe
4	7.2	0.096	Deflected Nappe

3. The height of the water surface and the profile of the flow for various discharges as obtained from experimental analysis were analyzed in Fluent by using User-Defined Function, with the use of macro generated based on the VOF - multiphase analysis.
4. The results obtained from the fluent solver simulations with multiphase model for both k-ε and k-ω are in good agreement with the experimental results as given in TABLE 3.

Table no 3 Comparative Results of free surface flow

S. No	Upstream depth (Y_1) in m			Downstream depth (Y_2) in m		
	Experimental Results	Simulation Analysis		Experimental Results	Simulation Analysis	
		k-ε model	k-ω model		k-ε model	k-ω model
1	0.2285	0.2285	0.229	0.0151	0.0159	0.0157
2	0.240	0.243	0.245	0.016	0.0163	0.0159
3	0.247	0.248	0.246	0.0208	0.0210	0.0213
4	0.252	0.249	0.251	0.022	0.0215	0.0217

5. The simulation results for all the four discharges are in good consonance with the experimental observations as depicted in the Fig. 7 below.

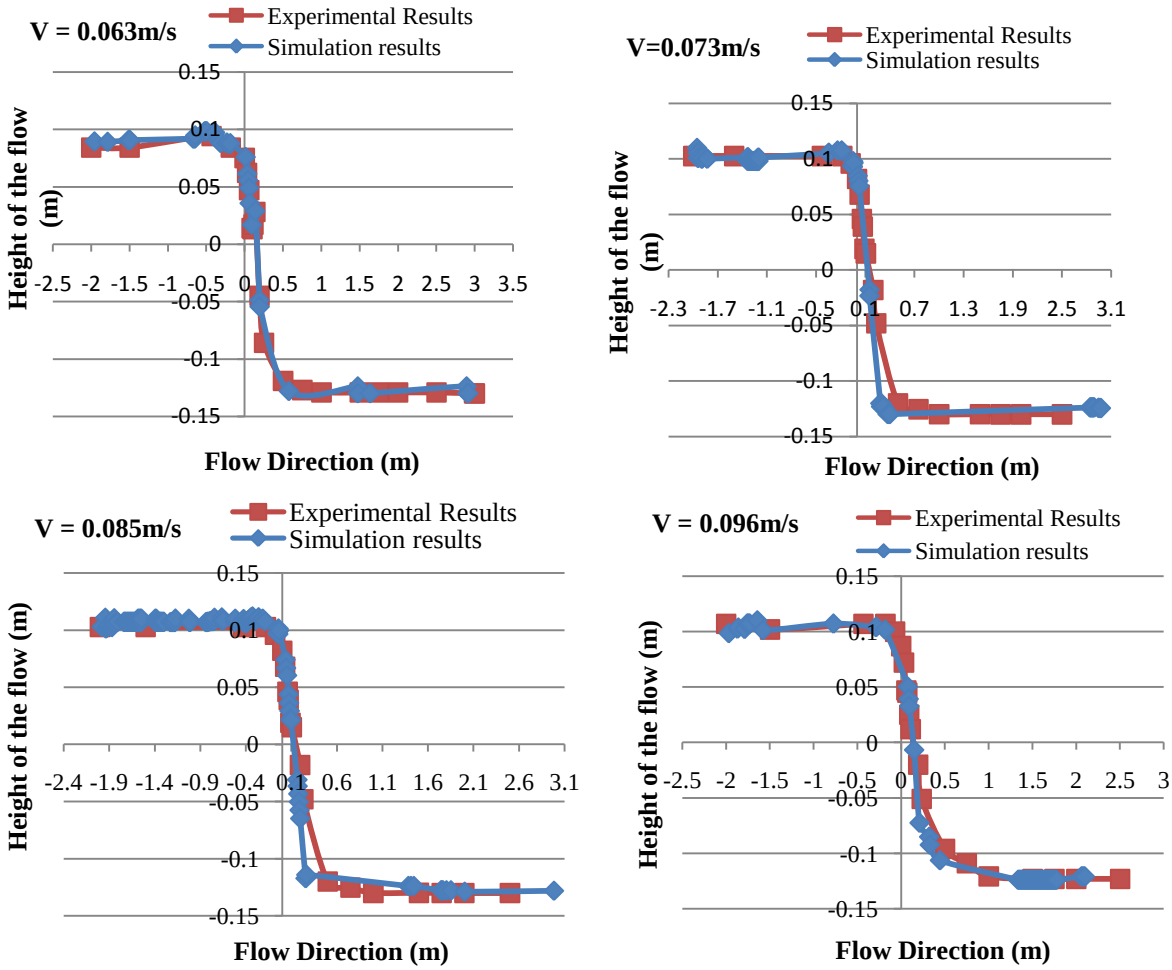

Fig no 7 Comparative Analysis of Flow Pattern

IV. Conclusion

Air-regulated siphons are very much useful as a means for safely disposing off the flood water to the downstream of the dam in the situations where manual interference is difficult. The present study was made to evaluate and emphasize that CFD analysis is an interesting and user friendly tool for simulation of complicated studies. For large and fine mesh cases, the simulation time step generally adopted is 0.001. Hence, the computational time is enormous. This is the prime limitation of the present study.

References

[1]. Bulu Atil, Spillways, in Water Resources, Civil Engineering Department, Hydraulics Division, Istanbul Technical University, 134 – 137.
[2]. Ervine, D. A., and Oliver, G. C. S., Full-scale behavior of air-regulated siphon spillway, Proc. Instn Civ. Engrs, Part 2, Glasgow University, 1980, 687-706.
[3]. Kay Melvyn, Practical Hydraulics, (Tailor & Francis, London and New York, 2008), 202-206.
[4]. Boatwright, Joshua, Air-Regulated Siphon Spillways: Performance, Modeling, Design, and Construction, doctoral diss., Clemson University, 2014.
[5]. Christopher R. Head, Low-Head Air-Regulated Siphon, Journal of Hydraulics Division, Proceedings of ASCE, 101(HY3), 1975.
[6]. Abdulnaser Sayma, Computational Fluid Dynamics, Venus Publishing ApS (www.bookboon.com), 2009
[7]. Wilcox, David C, Turbulence Modeling for CFD, DCW Industries, Inc. California, 2006.

Prasanna S V S N D L1 "Simulation of flows over an Air-Regulated Siphon Spillway." IOSR Journal of Mechanical and Civil Engineering (IOSR-JMCE) , vol. 15, no. 4, 2018, pp. 19-25